SYNTHESIS AND CHARACTERIZATION OF MULTIFERROIC CERAMIC $BaMn$O3 USING MIXED OXIDE SOLID STATE ROUTEN METHOD

[*]OWOLABI J. ADEYEMI[1]., ALI HARUNA[1]., SURAJU BALA[3]., UGBE RAPHEAL USHIEKPAN[1]., BEYIOKU DAVID[4]., HASSAN GAMBO MOHAMMED[1]., GODWIN AKONG OTU[2].

[1]Department of Physics, Nigerian Defence Academy, Kaduna
[2]Department of Computer Science, Airforce institute of Technology, Kaduna
[3]Department of Physics Umaru Musa Yaradua University, Katsina
[4]Department of Science Lab. Tech. Isah Mustapha Agwai 1 Polytechnic, Lafia

Abstract

This study relates to the conglomerate and structural properties of BaMnO3 oxide as a perovskite material prepared using the conventional solid-state reaction method. Perovskite structures have long been difficult materials to define new materials for use in many electronic applications such as actuators, switches, magnetic field sensors, and electronic memory devices. X-ray diffraction analysis measures and shows a diffraction pattern that shows a clear image at 1000x magnification on the fracture surface at a ratio of 1:1, 1:2, and 3:1. The peak positions and relative intensities of the X-ray diffraction pattern for a 1:1 ratio show that the synthesized BaMnO3 product is a single-phase perovskite oxide and has an orthorhombic structure with 304.61 Å and 3unit cell volume parameters of a = 6.434 Å , b = 5.316 A°, c = 8.906 A°. In the ratio of 1:2, the size of the BaMnO3 nanocrystal powder crystals is 40-45 nm. The most intense line is the Miller index with the values, 18.836 (003), 23.122 (112), 26.760 (022), 32.929 (222), and 35.652 (132) indicate that the synthesized BaMnO3 is a cubic crystal with a unit cell parameter of a = 9.415 Å. The 3:1 ratio indicates that the synthesized BaMnO3 is a tetragonal crystal with cell parameters of a = 9.431 A° and c = 37.774 A°, and the strongest lines and Miller indices for this structure are 24.147 (125), 26.696 (028). . , 32.856. (228), 38.138 (040) and 40.031 (1430). This result shows the spin of an electron in the field of spintronics, not the charge used to convey information.

Keywords: multi-ferroic, BaMnO3, X-ray diffraction analysis.

1.0 Introduction

New-generation energy-efficient devices have become the **focus** of modern technological **advances in** microprocessors, batteries and storage **devices.** The renaissance of multiferroic **materials is supported** by **new** discoveries and **concepts that** experimentally and theoretically

demonstrate a **wide** range of properties, including **magnetism** [1][2][3] ferro-electricity [4][5] **strongly** correlated **behavior of electrons** and magneto-resistance. [6][7] They **are** of interest to **scientists because of** their interesting multifunctional **properties.**[1].

The study of multi-ferroics is divided into several different areas, although the use of multi-ferroics in technology is currently a widely studied area. The physics governing magneto-electrical coupling in multi-ferroics is not yet fully understood. The ability to change the magnetization of a material by an applied electric field shows that less energy is consumed, so multi-ferroics can prove of great importance in the current field of research. However, in spintronics, electron spin is used to transfer information, not the charge. As a result, these devices can store information without an applied current, so they consume significantly less power than charge-based devices. The challenges associated with the use of multi-ferroics in the science and technology of perovskite oxides have resulted in the reduction of element sizes in microelectronic devices to the nano-scale. Because nanoscale perovskite oxides exhibit novel physical properties different from those of bulk, understanding the size effect of perovskite oxides at the nano-scale is important for developing novel electronic nano-devices. Because of these influences on structure and finite size, considerable efforts have been devoted to the controlled synthesis of low-dimensional perovskite nanostructures, such as perovskite oxide-based multi-ferrous materials, which are of great research interest due to their fundamental and technological significance. [8]. However, one major problem with these kinds of materials is that they generally exhibit anti-ferromagnetic order. Which have little or no magnetization and very few have been synthesized in the laboratory.

The magnetic ordering of this material arises from the interaction between the magnetic moments of adjacent spins, as described by the Heisenberg model, with Hamiltonian given by

$$H = -\sum J_{ij} S_i \cdot S_j \qquad 1.0$$

Here the J_{ij} value is called the exchange constant that describes the nature of the interaction between S_i and S_j. If J_{ij} is positive, the adjacent spins favor parallel alignment and the system is ferromagnetic. However, if J_{ij} is negative, the adjacent spins promote anti-parallel alignment and the system is anti-ferromagnetic. Antiferromagnetism can exist in many forms, with a common theme of moment been sublattices, arranged to cancel each other out and provide no net magnetization in the absence of an applied magnetic field. The system will be ferromagnetic if the sublattice is not equally opposed such that a net magnetization exists. [9].

In this regard, the proposed application field of materials of multifunctional electronic devices, for developing new multi-ferroic material such as $BaMnO_3$ of different stoichiometric ratios at high temperatures using conventional solid-state reaction methods for potential applications such as actuators, switches, magnetic field sensors or new types of electronic storage devices.

1.1 Solid State Reaction

The solid state reaction method is one of the commonly used preparation methods used to synthesize polycrystalline solids. In this reaction, the reactants react or diffuse chemically without the use of a solvent. It can also be called direct method or dry medium reaction. Standard chemical reactions are usually carried out at very high temperatures, ranging from 1000 to 1500 °C, by placing the reactants in a solvent before the reaction proceeds. These reagents react to form new substances. Because solids do not react with each other at ambient temperature, a chemical reaction proceeds at a significant rate and requires more time to heat to vapor temperature to achieve. After the reaction is complete, the new product can be removed from the solvent. Solid state reactions occur through solid state diffusion, which is the movement and movement of atoms without leaving the solid state. The diffusion process occurs mainly through lattice defects, voids and interstitial ions. It can also occur along grain boundaries, dislocations, inner and outer surfaces, etc. Diffusion along linear, planar, and surface defects was observed to be faster than 3D lattice in most cases. For this reason, they are also called high-diffusion paths or light-diffusion paths. In oxides and other inorganic compounds, temperature, partial pressure/activity of components, microstructure, particle size and porosity are some of the factors that influence the relative contribution to diffusion of various types. The method used to prepare the solid precursor and the pretreatment received prior to the reaction greatly affect reactivity. The size and shape of the constituent particles of the precursor powder have a distinct effect on the reaction rate. In addition, the degree of accessible surface influences the nucleation of the crystal and the geometry of interface development. [10][11].

2.0 Methodology

2.1 a. Raw materials

$BaCO_3$ Powder, MnO_2 Powder, Toluene, Acetone, Polyvinyl Alcohol, Distil Water.

b. Apparatus

Weighing balance, Motor and Pestle Agea, Glass Wire, Hydraulic Press, Furnace Crucible Lid

Table 1.0: Stochiometric calculation of Precursor Mass of BaMnO3

S/N	Ratio	Precursor	Molar Mass	Mass (g)
1	1:1	$BaCO_3$	197.335	20.05
		MnO_2	86.936	20.04
2	1:2	$BaCO_3$	197.335	20.05
		MnO_2	86.936	40.08
3	3:1	$BaCO_3$	197.335	60.05
		MnO_2	86.936	20.04

2.2 Synthesis Procedure of BaMnO3 solution

For the synthesis of a strong BaMnO3 solution, a weighing balance was used for the starting material by weighing the BaCO3 and MnO2 powders shown in Table 1.0 in stoichiometric ratios of 1:1, 1:2 and 3:1 mol. and wet mixing of the powder with acetone within 2 hours. The mixture was grinded for 60 minutes using an agate mortar and pestle. Before mixing, barium carbonate was dried at 180° C. in an oven, mixed with manganese dioxide, and heated to 800° C. for 6 hours to remove moisture. The transformed powder mixture is calcined at 900 °C for 6 hours. Calcination is a high-temperature treatment method prior to sintering. The calcined powder is grinded using a ring mill and properly mixed with polyvinyl alcohol, which acts as a binder and imparts some mechanical strength to the pellets made from it. It also reduces the brittleness of the granules and the duration of particle formation. This sample was modified and then ground for a period of time at t = 1, 2, 3, 4, 5, and 6 h. After grinding, the sample turned into a compressed one. About 1-2mm thick cylindrical pellets had been prepared from the powders via the use of a hydraulic press at 15 tones. The pellets had been sintered at 1100^{o}C for 6 h. Sintering is the warm temperature treatment method after calcination when, the body is heated at a temperature above 1000^{o}C for 6 hours. During this firing stage, diffusion of atoms takes vicinity amongst powder particles and the powders are consolidated and the specimen shrinks, and emerge as a dense material. Fig. 2.0: Shows the Schematic diagram for the synthesis of $BaMnO_3$ using solid state reaction

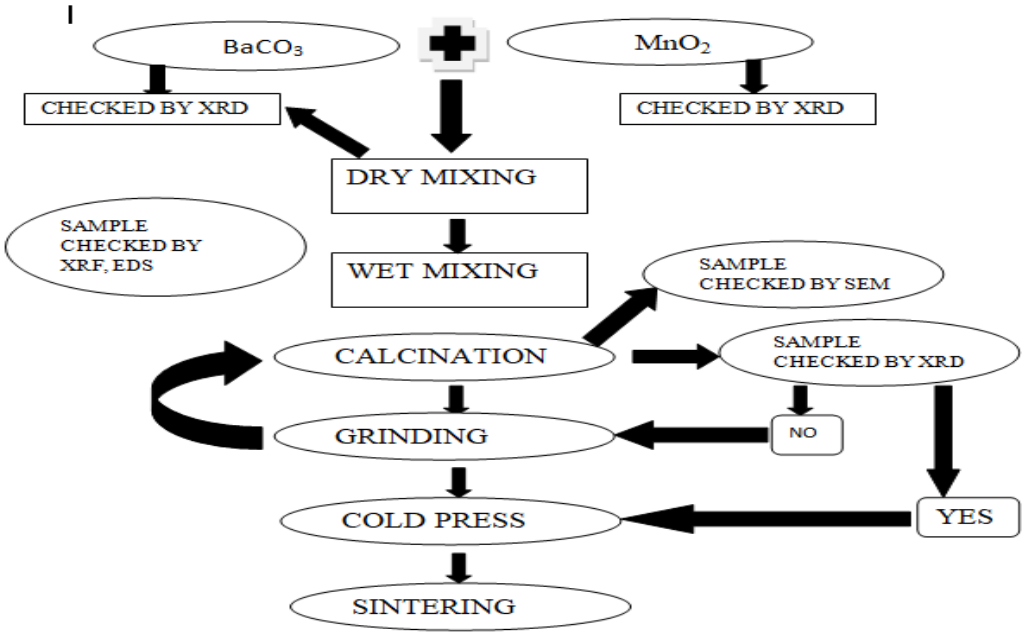

Fig 2.0SCHEMATIC DIAGRAM FOR THE SYNTHESIS OF BaMnO3 USING SOLID STATE REACTION

2.3 Characterization Method

Phase analysis of calcined BaCO3 and MnO2 powders in 1:1, 1:2 and 3:1 molar ratios in this study was characterized by X-ray diffraction (XRD). X-ray diffraction (XRD) of a BaMnO3 multi- ferroic sample was prepared at 1000 °C for 6hours using a D5000 diffractometer with a Cu Kα at (1.5418 Å) radiation source and a nickel Kβ filter operating at 40 kV and 30 mA was selected and characterized for structural and morphological property.

XRD data were collected in the range of range 2θ = 10°–90°, in 0.02°/min increments. The microstructure of the sample was analyzed using a scanning electron microscope (SEM) at an acceleration voltage of 10 kV. To identify the resulting BaMnO3 compound, samples of the resulting compound were recorded by energy dispersive X-ray spectroscopy in 200-800 nm wavelength range. BaSO4 was used as the reference material for baseline calibration.

Figure 2.1.1a – 2.1.1c show the morphology of BaMnO3 by scanning electron microscopy (SEM) in different ratios of 1:1, 1:2, and 3:1 at x1000 magnification.

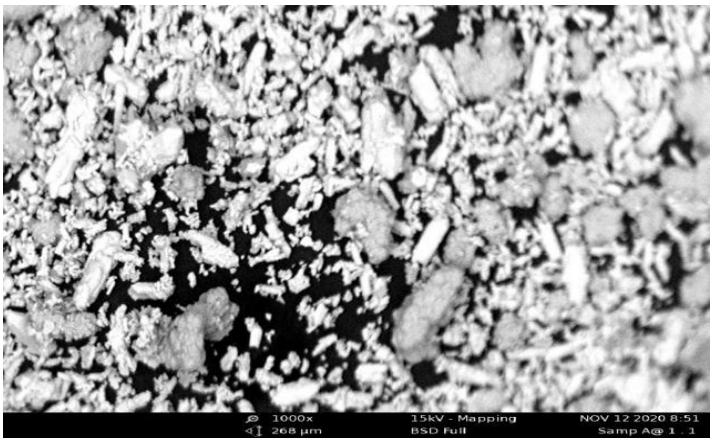

Fig.2.1.1a. Scanning Electron Microscopy of$BaMnO_3$ of ratio 1:1 (x1000) magnification

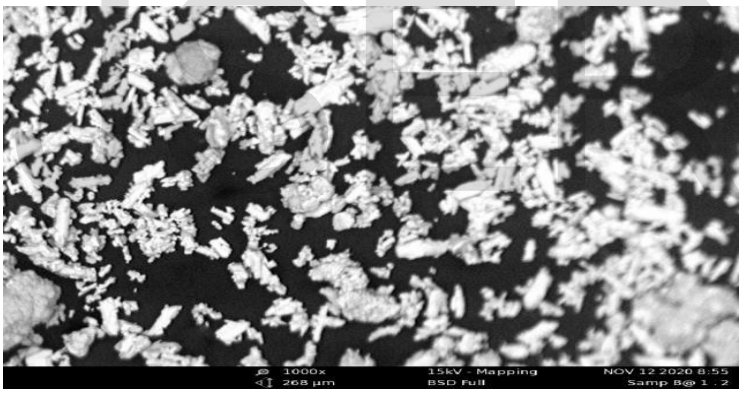

Fig.2.1.1b. Scanning Electron Microscopy of$BaMnO_3$ of ratio 1:2 (x1000) magnification

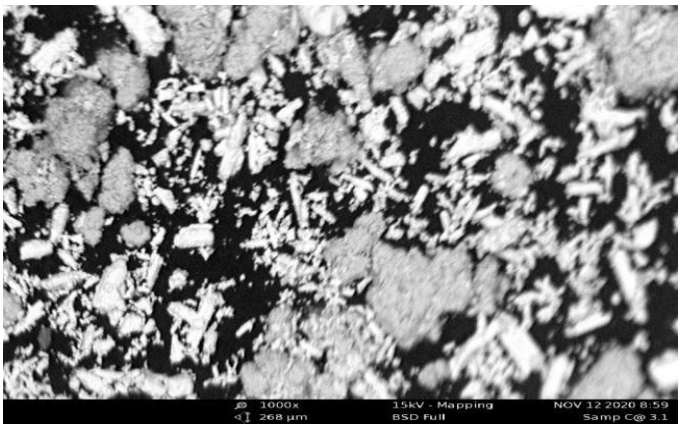

Fig.2.1.1c. Scanning Electron Microscopy of$BaMnO_3$ of ratio 3:1 (x1000) magnification

3.0 RESULTS AND DISCUSSIONS

In this research, our results is divided into four part which include the synthesis of $BaMnO_3$ multiferroics material, scanning electron microscopy (SEM) analysis, X-Ray Diffraction (XRD) analysis and Energy Dispersive X-ray Spectroscopy (EDXRF) analysis.

The SEM morphology in Figure 2.1.1(a-c) shows a clear image with magnification of ×1000for fractured surfaces at ratio 1:1, 1:2, 3:1. From this illustration, the SEM morphology of the sample synthesized at the optimum reaction temperature and time is 1000 ^oC and 6h.

Fig.2.1.1a: describes the morphology of the grain powder at ratio 1:1; this shows an irregular smooth and tiny surface with a small traces and very low roughness of fresh substrates with low porosity and average diameter of 268nm with the particle sizes in the range of 0.5–3nm of BaMnO3. This confirms the nanometric sizes of the samples. In addition, it shows that the size of the crystallites at the same ratio has good results for equal proportion of the sample.

Figure 2.1.1b; describes SEM images of $BaMnO_3$ powder at ratio 1:2; this shows a diffusion of the materials with homogeneous agglomerates made of man-sized crystallites ranging from 70 and 110 nm over the reduction of roughness as the thickness of the film increases which were confirmed from the strong peaks of the XRD pattern.Uncertainly the size of the particles increases little by the increase at the calcination temperature. This nano-sized powder has a high porosity. The force responsible for agglomeration process which tends to reduce the surface energy is the Van der Waals forces.

Figure 2.1.1c; shows SEM images of $BaMnO_3$ powder shape, size and different morphologies at ratio 3:1. During the synthesis process, the reaction condition was varied by using different surfactants which shows the rapid diffusion of the incoming material with a roughness of 2nm.

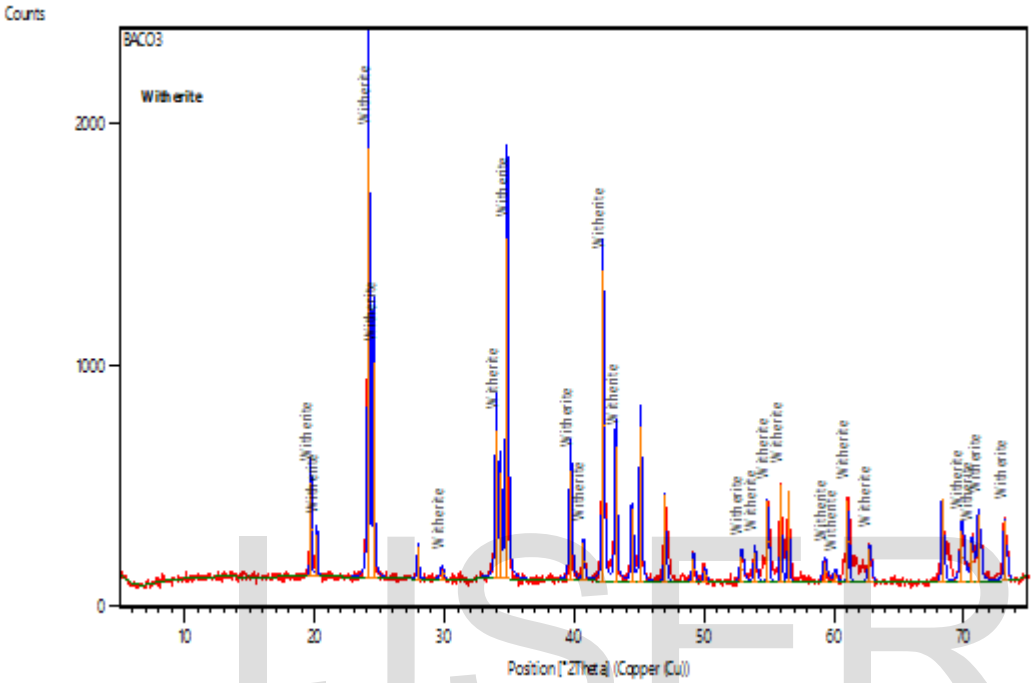

Fig: 3.0: The Diffractogram Graphics of $BaCO_3$

Figure 3.0 shows the sharp diffraction peaks of the sample which indicates that a crystallized $BaCO_3$ crystal can be easily obtained under current synthetic condition. Since there are no characteristic peaks of other impurities been detected, this indicates that the products are of high purity. The broadening of the peaks indicates that the particles were of nanometer scale while the width of the strongest peak decreases with increasing of the calcinations temperature, which refers to the growth of crystal size.

Also the intensity of the peaks increases with increasing calcination temperature, which leads to more crystalline structure [9]. Where θ is the Bragg angle of diffraction lines, K is a shape factor taken as 0.9, λ is the wavelength of incident X-rays (λ=0.154056 nm), and β is the full-width at half maximum (FWHM).

In addition, the mean crystallite sizes increase with the increasing of the calcination temperature, which refers to the more crystalline structure.

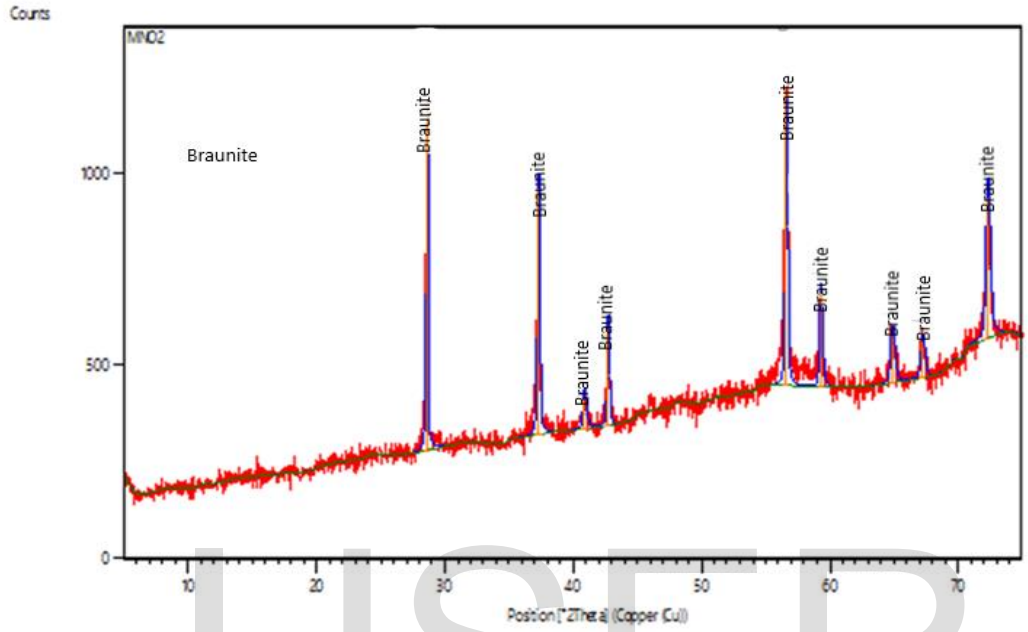

Fig: 3.1: The Diffractogram Graphics of MnO_2

Figure 3.1 indicate that the MnO_2 nanowires grow in the [0 0 1] direction and that the rough surface of figure 3.1.1b is parallel to the (2 1 0) plane. The sample shows high purity of MnO2 as indicated by the X-ray diffraction (XRD) pattern. MnO2 has a tetragonal Hollandite-type structure with space group I4/m, in which the MnO6 octahedral are linked to form double zigzag chains by edge-sharing.

These double chains then share their corners with each other forming approximately square tunnels of MnO2 nanowires which are expanded due to high density of defects in the nanostructures.

Furthermore, the peak of the sample is obviously higher than the peak in the standard polycrystalline diffraction. This confirmed the conclusion deduced from the pattern. The valence state of Mn is very flexible from 0 to 27 because of its valence shell configuration of $3d^5\ 4s^2$.

For the MnO2 with nano wire structure in this work, the phase has been confirmed as high purity of MnO2 by XRD.

3.2 Diffraction pattern measurements

Figure 3.1.1a-c visualize the diffraction measurements at ratio 1:1, 1:2 and 3:1 of BaMnO3. This diffraction measurement indicates a diffraction pattern which is also called a *powder pattern*. In a standard diffraction patterns, the X-axis is 2θ in degrees and the Y-axis is the intensity of diffraction. Following Bragg's Law, *d*-value is infinite at 0^{o} 2θ but decreases quickly with increasing angle.

The peaks in Figure 3.1.1a-c are called reflections, and are labeled with the 2θ angles at which diffraction occurs. They are also labeled with associated *hkl* indices, called *Laue indices*, and *d*-values. But By convention, when looking at diffraction directions, we use Laue indices with no parentheses because we are labeling a reflection and not a family of planes as is done in this figures.

According to Bragg's Law, Figure 3.1.1a has a stronger peak intensity of 26.0^{o} at 2θ and a strong peak intensity of 35^{o} and 45 which shows that it is a high symmetry system with identical planes of atoms in the same ratio correspond to large *d*-values. The large values are due to the layered atomic arrangements. The Peaks position and relative intensities of the XRD pattern indicates that the synthesized product $BaMnO_3$ was a single phase perovskite-type oxide which consist of orthorhombic crystal structure with 304.61 A˚ of 3 unit cell volume and cell parameters of a = 6.434 A˚ , b = 5.316 A˚ , c = 8.906 A˚ at ratio 1:1. As shown from XRD structure.

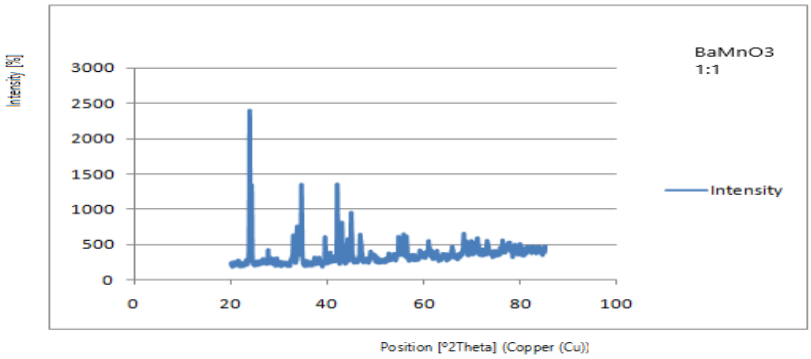

Fig.3.1.1a. X-ray diffraction pattern of BaMnO3 at 900^{o}c room temperature of ratio 1:1

In Figure 3.1.1b, Different minerals produces different diffraction patterns because patterns depend on mineral composition and on the locations of atoms in the unit cells. So, space symmetry, which relates to atomic location, has great influence on the diffraction patterns.

Figure 3.1.1b shows two strong peaks intensities at 26 degree and 36 degree due to the increase in the MnO_2 and a slight increase of its intensity at a lower peak of 59, 70 and 85 degrees.This may be due to the first-order diffraction in the planes with decreasing d-value. Although, Higher-order diffraction from other families of planes, too, can cause diffraction at this angles.With the increase of Mn compound, the position of diffraction peak in the XRD pattern shifted slightly tothe right, indicating that the value of 2θ increased while the value of D interplanar spacing decreased, so the cell parameters of the sample decreased slightly with the increase of Mn compound, and the crystal surface spacing decreased, indicating that Mn3+ with relatively small radius successfully entered the perovskite lattice, partially with relatively large radius.

The crystallite size of $BaMnO_3$ nanocrystals powder was in the range of 40–45 nm. The most intensive peak lines Miller indexes are; 18.836(003), 23.122(112), 26.760(022), 32.929(222) and 35.652(132) which indicate that the synthesized $BaMnO_3$ was a cubic crystal structure with cell parameters of a = 9.415 A˚ at ratio 1:2.

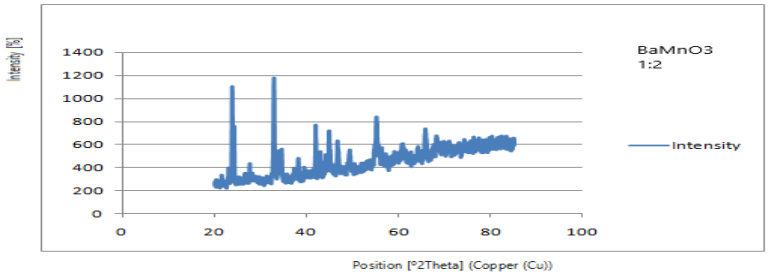

Fig.3.1.1b. X-ray diffraction pattern of BaMnO3 at room temperature of ratio 1:2.

Figure 3.1.1c shows a very strong intensity peak at 26 degree and two lower peaks at 36 and 45 degree due to increase in BaCO3. Following Bragg's Law, *d*-value decreases quickly with increasing angle. With the increase of BaCO3 the average particle size of the sample decreases gradually, which indicates that the BaCO3 is beneficial to reduce the particle size of the sample.

However, when the amount of BaCO3 increases, the average particle size also increases, indicating phase production in the synthesis process, which makes the sample a mixture, thus affecting the distribution of the particle size.

The most intensive lines and Miller indexes for this pattern is 24.147(125), 26.696(028), 32.856(228), 38.138(040) and 40.031(1430 which indicate that the synthesized $BaMnO_3$ at 3.1 was a Tetragonal crystal structure with cell parameters of a = 9.431 A˚ and c = 37.774 A˚ at ratio 3:1.

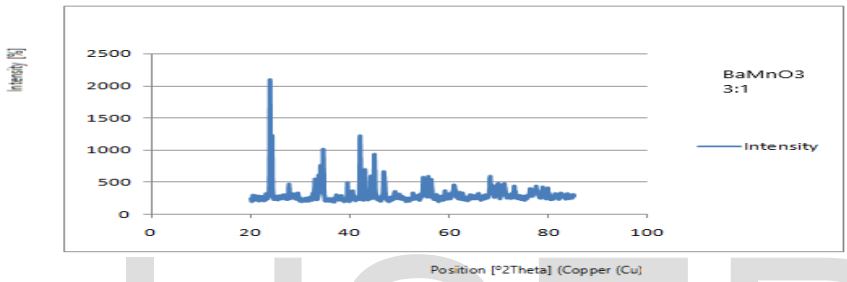

Fig. 3.1.1c.X-ray diffraction pattern of BaMnO3 at room temperature of ratio 3:1

4.0 SUMMARY AND CONCLUSION

In this research, BaMnO3 the multiferroic ceramic oxide has been prepared using solid state reaction route technique. The diffraction pattern structures were obtained using the X-ray diffraction (XRD), and the structural morphology was obtained using micro-structural (SEM). Based on the results obtained, the X-ray diffraction pattern of ratio 1:1 of BaMnO3 shows that this compound is single phase oxides which consist of orthorhombic crystal structure. While ratio 1:2 indicates that BaMnO3 is a cubic crystal structure and ratio 3:1 indicate BaMnO3 was a Tetragonal crystal structure. Scanning Electron Microscope (SEM) shows the crystallinity and

homogeneity distribution of grains, ranging from 1-1.5μm. The compound in this research is well sintered and densely packed.

REFERENCE

1. Kingery, W.D., Bowen, H.K. and Uhlmann, D.R. (1976) 'Introduction to Ceramics', 2nd Edn., Wiley, New York,.
2. Moulson, A.J. and Herbert, J. M. (2003). 'Electroceramics', Second Edition, John Wiley and Sons Ltd, England.
3. Constantinescu, D.M., Sandu, M., Volceanov, E., Miron, M.C. and Apostol, D.A.(2009) "Strength Response and Failure Analysis of Ceramic Alumina Tiles", Key Engineering Materials, 417-418, pp. 673- 676,.
4. Babalola, O.A., Alabi, A.B. and Akomolafe, T. (2010) "Microsructural Analysis of Zinc-Clay Cermet Resistors", Researcher, 2, pp. 48-55,.
5. Wiebe C.R., Greedan J.E., Kyriakou P.P., Luke G.M., J.S. Gardner J.S., Fukaya A., GatMalureanu I.M, Russo P.L., Savici A.T., Uemura Y.J, (2003) "Glasslike ordering and spatial inhomogeneity of magnetic structure in Ba3FeRu2O9: Role of Fe/Ru site disorder", Phys. Rev. B, 68, pp. 134410.
6. Li M., Pietrowski M.J., De Souza R.A., Zhang H., Reaney I.M., Cook S.N, Kilner J.A.,Sinclair D.C, (2014) "A family of oxide ion conductors based on the ferroelectric perovskite Na0.5Bi0.5TiO3', Nat. Mater. 13, pp. 31.
7. Cheong S.W., M. Mostovoy M., (2007) "understanding multiferroic Hexagonal Manganites by Static and Ultrafast Optical Spectroscopy", Nat. Mater. 13, pp. 5-31.
8. Jaap F. Vente. (2001) Structural and magnetic properties of layered Sr (7) Mn (4) O (15). Physical Review B, 64(21) DOI: 10.1103/Physical Review B.64.214403.
9. Blundell, S. (2001). Magnetism in Condensed Matter. Oxford University Press.
10. Oliveira, G.N.P., Araújo, J.P and Lopes A.M.L (2017) Local probing spinel and perovskite complex magnetic systems
11. BamfordC. H. (1980). Comprehensive Chemical Kinetics, Vol. 22 of Reactions in the Solid State, Elsevier Scientific